Microchemical Journal 143 (2018) 252–258

Contents lists available at ScienceDirect

Microchemical Journal

journal homepage: www.elsevier.com/locate/microc

Structural analysis of natural deep eutectic solvents. Theoretical and experimental study

Pablo L. Pisano[a,*], Magdalena Espino[b], María de los Ángeles Fernández[b], María F. Silva[b], Alejandro C. Olivieri[a]

[a] Departamento de Química Analítica, Facultad de Ciencias Bioquímicas y Farmacéuticas, Universidad Nacional de Rosario, Instituto de Química Rosario (IQUIR-CONICET), Suipacha 531, Rosario S2002LRK, Argentina
[b] Instituto de Biología Agrícola de Mendoza (IBAM-CONICET), Facultad de Ciencias Agrarias, Universidad Nacional de Cuyo, Mendoza, Argentina

ARTICLE INFO

Keywords:
Natural deep eutectic solvents
Green analytical chemistry
Nuclear Overhauser effect
Nuclear magnetic resonance
Density functional theory

ABSTRACT

A theoretical and experimental study was performed on natural deep eutectic solvents (NADES) formed by lactic acid-glucose (LGH), citric acid-fructose (CFH) and citric acid-glucose (CGH). The presence of nuclear Overhauser effect (NOE) in the proton nuclear magnetic resonance (^{1}H NMR) spectra of the NADES was studied. The spatial proximity between the NADES components was experimentally confirmed by the detection of multiple NOE effects in the dilutions analyzed. LGH showed the best outcome by partially maintaining its supramolecular structure throughout the dilutions. In order to rationalize the intermolecular interactions generated among the components, a theoretical study was performed using a density functional theory (DFT) computational method. A simplified dimeric model of the NADES was selected in order to achieve a rapid screening of the system searching for interactions between their constituents. In agreement with the experimental evidence, the calculations allowed to confirm the spatial proximity, by finding at least two hydrogen bonds between the components of every NADES.

1. Introduction

The development of sustainable solvents represents one of the main challenges of Green Analytical Chemistry. In this context, Natural Deep Eutectic Solvents (NADES) have been introduced as a green alternative to ionic liquids (ILs) due to their environmental friendly composition, ease of preparation, low cost and biodegradability. NADES are eutectic mixtures constituted by metabolites naturally present in all types of cells and organisms. The common components are sugars (glucose, sucrose, fructose, etc.); organic acids (lactic, malic, citric acids, etc.); urea and choline chloride [1]. A eutectic system is a combination of substances building a super-lattice that melts and freezes at a temperature that is lower than the melting points of the separate constituents, being hydrogen bonding and Van der Walls interactions the main driving forces of this phenomenon [2,3]. There are four methods available for preparing NADES (a) heating and stirring method [4]: the components are placed in a bottle with a stirring bar and cap and heated in a water bath with agitation till a clear liquid is formed; (b) evaporating method [4]: components are dissolved in water and solvent evaporated with a rotary evaporator, the liquid obtained is placed in a desiccator with silica gel till constant weight; (c) freeze-drying method [5] based on the freeze-drying of aqueous solutions of the individual counterparts; (d) microwave assisted preparation [6]: the component mixture is microwave irradiated at low power during a few seconds.

The physicochemical properties of the eutectic mixture (viscosity, conductivity, density and polarity) depend on the chemical nature of its components and on their intermolecular interactions [7]. The hydrogen bonding interactions lead to highly structured liquids. Interestingly, NADES can form additional hydrogen bonds with solutes, which gives rise to endless analytical applications [4,8–10]. Thus, NADES components can be tailored to be target-specific. Unique interactions between the NADES with target analytes make possible to selectively separate trace compounds from complex matrices [11,12]. NADES physicochemical properties can be modified with water addition, in order to lower viscosity and density or increase their polarity. However, it has been reported that dilution around 50% caused progressive rupture of the hydrogen bonds and even the loss of the intermolecular interactions [11].

In recent years, some reports exploring the structure of NADES formed mostly by choline chloride have appeared [4,11,13]. To the best of our knowledge, although NADES formed by monosaccharides (glucose, fructose) and organic acids have been explored for their

* Corresponding author.
E-mail address: pisano@iquir-conicet.gov.ar (P.L. Pisano).

https://doi.org/10.1016/j.microc.2018.08.016
Received 14 March 2018; Received in revised form 9 August 2018; Accepted 10 August 2018
Available online 11 August 2018
0026-265X/

interesting analytical applications [14–16] there are no reports of their intermolecular interactions and the influence of its dilution.

In most NMR experiments, the spectra are obtained by interactions of the nuclei through bonds (scalar or *J*-coupling). When nuclei interact with each other directly through space (dipolar or magnetic coupling), a phenomenon responsible for the nuclear Overhauser effect (NOE) takes place. In NOE experiments, one proton in the molecule is irradiated immediately before the acquisition of the spectrum, creating a magnetization on that proton alone in the molecule. After this selective excitation, there is a waiting period called mixing time, in which transfer of magnetization to other protons (the increase of the NOE effect) leads to a small but measureable enhancement in the signals of any other peak that corresponds to protons nearby in space [17].

The aim of this work was to perform an experimental and theoretical study of the NADES formed by lactic acid-glucose-water (LGH), citric acid-glucose-water (CGH) and citric acid-fructose-water (CFH), in order to rationalize the intermolecular interactions generated among the components. To this end, the existence of the NOE effect in the ^{1}H NMR spectra of the NADES was studied. Furthermore, NADES constituents were modelled with a density functional theory (DFT) computational method. In addition, we studied different dilutions of NADES and their interaction with analytes, with the purpose of exploring the effect produced on the modification of the supramolecular structure.

The results indicate that strong NOE interactions of the hydrogen bonding type, with distances in the range 1.71–2.75 Å, were observed in the three analyzed NADES. Furthermore, each NADES presents at least two hydrogen bond interactions. Interestingly, dilution effects in the structure showed in some cases that water solutions that contain up to 20% of NADES partially maintained their supramolecular structure, as confirmed by the presence of the NOE interaction.

2. Material and methods

2.1. Reagents and standards

All reagents and solvents were used directly as purchased or purified according to standard procedures [18]. The absence of impurities was verified in the ^{1}H NMR spectra due to the lack of isolated signals not belonging to the NADES mixtures. Compounds for NADES preparation including glucose anhydrous (99%), citric acid anhydrous (99%), D-(−)-fructose (99%), L-(+)-lactic acid (85–90%) were purchased from Biopack (Bs. As., Argentina). Quercetin dihydrate (QR, 3,3′,4′,5,7-pentahydroxyflavone) 97% was obtained from Alfa Aesar (Haverhill, MA, USA). Ultrapure water was obtained from a Milli-Q system (Millipore, Billerica, MA, USA). Deuterium oxide (D_2O, deuterium degree 99.9%) and 3-(trimethylsilyl) propionic-2,2,3,3-d_4 acid sodium salt (TMSP, deuterium degree 98%) were purchased from Sigma-Aldrich.

2.2. NADES preparation

NADES were prepared using a method previously described by Dai and co-workers [4]. The component mixture LGH (lactic acid:glucose 5:1); CGH (citric acid:glucose, 1:1) and CFH (citric acid:fructose, 1:1) were placed with 15% of H_2O (v/v) in a 20 mL amber glass vial. Subsequently, the mixture was heated in a magnetic stirrer with temperature control (Fisatom model 752A, Brasil) at 80 °C for 60 min. The synthesized NADES were transferred under nitrogen flow to completely fill amber glass vials, and stored at 4 °C to ensure their preservation until NMR analysis. Dilutions from 50 to 90% of the corresponding NADES were prepared by adding the necessary amount of D_2O and water to the original mixture, e.g., 10% LGH were constituted with 90% water and 10% of LGH. In the case of the LGH interaction with QR, the analyte was added to the LGH dilutions, to reach a 10 mg L^{-1} QR solution in the corresponding NADES dilution.

2.3. NMR spectroscopy

All NMR spectra were recorded on a 300 MHz Bruker Avance spectrometer with a frequency and a phase resolution of 0.005 Hz and 0.006° respectively, fitted with an autosampler with a 5 mm internal diameter smart probe with ATMA (Automatic Tuning Matching) [19]. During the experiments, the temperature was held stable at 300 K. Each sample was acquired in triplicate. The D_2O was used as the field frequency lock signal, TMSP for internal referencing of ^{1}H chemical shifts. Suppression of H_2O signals was carried out by using noesygppr-1d (Bruker standard pulse sequence). Each spectrum was recorded with 128 scans and 48 K data points. The spectral width was adjusted to 15.0084 ppm (4504.504 Hz) with an acquisition time of 4.0 s per scan. The NOE spectra were performed by irradiating the particular proton signal under study with a spectral width between 25 and 45 Hz (0.08 and 0.15 ppm, respectively), depending on the signal. Subsequently, NOE difference spectra were calculated by subtracting original ^{1}H NMR of the corresponding NADES from the irradiated ^{1}H NMR spectrum.

2.4. Computational methods

Initially, molecular modelling of the systems begun with conformational searches that yielded a large number of geometries (up to 100) of the NADES constituents (glucose, fructose, lactic acid and citric acid) with the molecular mechanics method MM+ using the conformational search module of the HyperChem package [20]. Subsequently, the most stable conformations were optimized with the M06-2X exchange correlation functional [21] coupled with the 6-31 + G(d,p) basis set by using the Gaussian 09W program [22]. The functional M06-2X from Truhlar's group is frequently used to model non-covalent interactions [23].

While the stoichiometry relationship between organic acid and carbohydrates in NADES preparation was 5:1 (LGH) or 1:1 (CGH and FCH), when three systems of these sizes (more than 25 heavy atoms) are modelled, the CPU calculation times become prohibitively long for a rational design. Consequently, the model chosen for the tree systems under study was a dimer containing one molecule of organic acid and one molecule of sugar. Although a dimer model cannot describe thoroughly all possible stabilizing intermolecular interactions between the NADES components, this simplified model of the NADES was selected in order to achieve a rapid screening of the system searching for interactions between their constituents. Accordingly, intermolecular interactions in the NADES were modelled by placing the most stable conformations of the constituents at a distance of approximately 3.5 Å, and re-optimizing the geometry of the system in water (ε = 78.3553) with the method M06-2X/6-31 + G(d,p). For these solvent optimizations, Solvation Model based on Density (SMD) [24] of the Self-Consistent Reaction Field method (SCRF) [25] was used. Finally, frequency calculations were performed to verify the nature of the stationary points (global energy minima) by the absence of imaginary frequencies in all the optimized structures. In order to examine the more important interactions in the modelled systems we performed natural bond orbital (NBO) calculations and Wiberg bond indexes were analyzed [26]. Reported thermochemical properties include zero-point energies (ZPEs) without scaling and were calculated at 1 atm and 298.15 K.

3. Results and discussion

3.1. Experimental study

3.1.1. Nuclear Overhauser effect in NADES

In a first phase, LGH, CFH and CGH were analyzed by ^{1}H NMR in order to select the hydrogen atoms that were eligible for NOEs experiments, namely protons with chemical shifts different enough (at least in 0.3 ppm) from the remaining protons in the other molecules that conform the mixture. This requirement is due to the fact that the

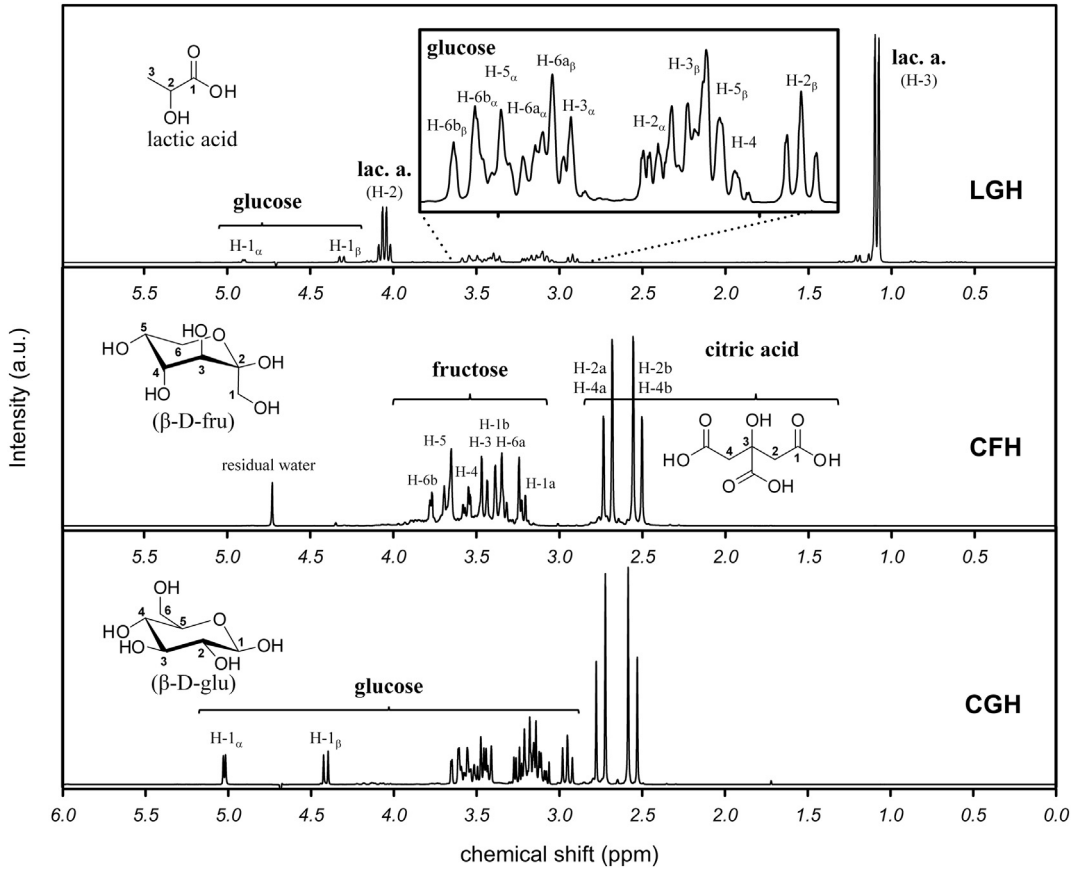

Fig. 1. ^{1}H NMR spectra of the NADES under study. LGH: lactic acid-glucose, CFH: citric acid-fructose, CGH: citric acid-glucose. lac. a.: lactic acid, β-D-fru: β-D-fructopyranose, β-D-glu: β-D-glucopyranose.

hydrogen selected for irradiation should respond in an isolated region of the spectrum, to prevent other protons reaching magnetization, which would lead to wrong conclusions in the analysis.

As shown Fig. 1, both signals from lactic acid (H-2 and H-3) appear clearly separated from glucose signals in LGH. In case of CFH and CGH, double-doublet from citric acid (H-2a, b and H-4a, b) appear separated from sugar signals. Therefore, the signal selected for NOE experiments in the NADES containing citric acid (CFH and CGH) was the doublet at δ = 2.7 ppm (first doublet from the double-doublet), while for LGH, the two signals selected for irradiation were the quartet at δ = 4.10 ppm and the doublet at δ = 1.20 ppm from lactic acid (H-2 and H-3, respectively). In addition, all ^{1}H NMR spectra were also irradiated in the central region of the sugar moieties, corresponding to the chemical shifts from most carbinolic protons (i.e., around δ = 3.30 ppm for glucose and δ = 3.60 ppm for fructose).

Structures of major isomers of D-fructose and D-glucose are also shown in Fig. 1. At equilibrium in water β-D-fructopyranose (Fig. 1, β-D-fru) is the preponderant tautomer of D-fructose, followed by β-D-fructofuranose, and then α-D-fructofuranose (69.6%, 21.1% and 5.7% respectively) [27,28]. In case of D-glucose, pyranose were clearly the predominant forms (c.a. 99% in a 36:63 ratio for α:β anomers respectively) [29]. Although mayor isomer of D-glucose in water is β-D-glucopyranose (Fig. 1, β-D-glu), integration of anomeric H-1 signals (H-1$_\alpha$ and H-1$_\beta$) afforded a relationship close to 1:1 between the glucopyranose anomers for the CGH mixture. In the latter case, it seems that the formation of the NADES altered the original equilibrium.

Fig. 2 summarizes the best NOEs found for the three NADES under study. In LGH, when both signals from lactic acid were irradiated, the most intense NOEs were recorded by the irradiation of H-3 from lactic acid. As can be seen in Fig. 2a, the existence of NOE was confirmed by the occurrence of signals corresponding to most of the carbinolic glucose hydrogens in the ^{1}H NMR spectrum (H-2, H-3, H-5 and H-6). Furthermore, with the irradiation at the central region of glucose protons (H-3, H-5 and H-6), the appearance of both H-2 and H-3 signals from lactic acid was observed in the ^{1}H NMR spectrum.

In the case of CFH, when the selected signal was irradiated (δ = 2.7 ppm), the existence of the NOE effect was observed by the occurrence of signals corresponding to most of the fructose carbinolic hydrogens in the ^{1}H NMR spectrum (H-1, H-3, H-4, H-5 and H-6, Fig. 2b).

Finally, Fig. 2c shows the NOEs generated when the selected protons of CGH were irradiated. Through irradiation of the signal at δ = 2.7 ppm, most of the glucose carbinolic hydrogens (H-2, H-3, H-5 and H-6) emerge in the ^{1}H NMR spectrum. Furthermore, since in this case the region of the ^{1}H NMR spectrum for protons attached to the anomeric carbons (H-1$_\beta$) is clear, it was also possible to see the NOE effect in these signals. In addition, a reciprocal NOE was detected when we irradiated the central region of glucose protons, i.e., the occurrence of the proton signals from citric acid was observed in the ^{1}H NMR spectrum.

Unfortunately, NOEs intensities compete with a relaxation process that returns all of the protons to the equilibrium state. The rate of the relaxation process is determined by how fast the molecule as a whole tumbles or rotates in solution. Since small molecules relax more slowly than large molecules, they require longer mixing times to capture the strongest NOE enhancements. Accordingly, for small molecules in non-viscous solvents, the optimal mixing time in a NOE experiment can be as long as 1.5 s, and for large molecules in more viscous solvents, the best setting can be ca. 0.15 s. Therefore, once we had the preliminary results of the existence of NOEs in the NADES solvents, three different NOE experiments for LGH mixture were carried out with 0.15 s, 0.7 s and 1.5 s mixing times respectively, in order to study the influence of

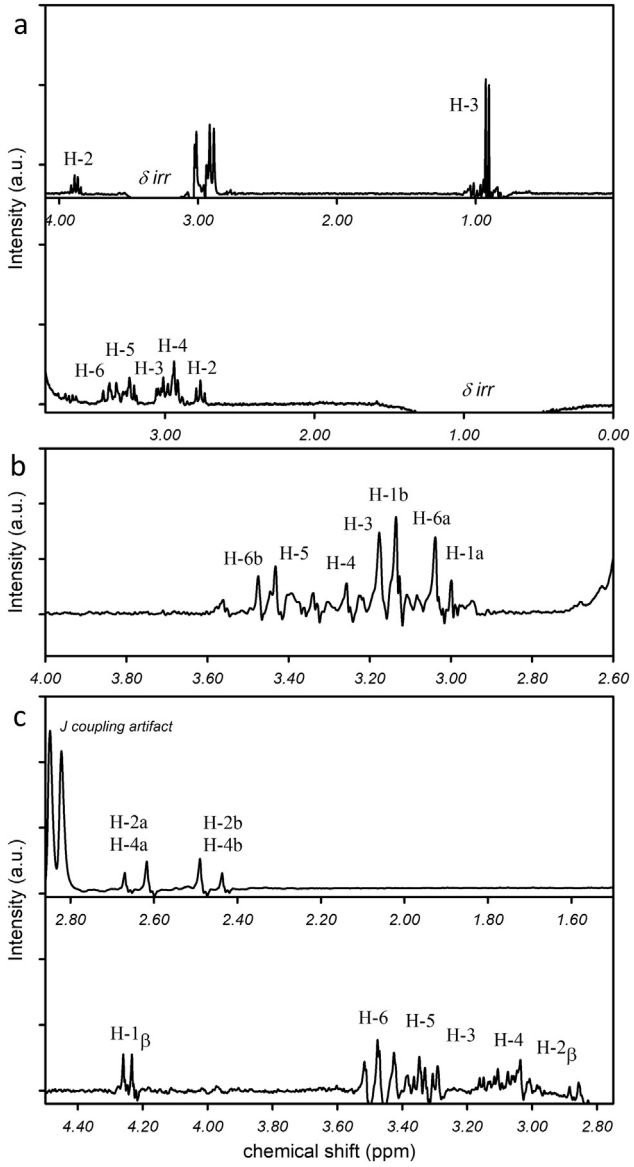

Fig. 2. NOE difference spectra registered from the ^{1}H NMR spectra of the NADES under study. a) Irradiation at δ = 1.2 ppm and δ = 3.6 ppm signals in LGH. b) Irradiation at δ = 2.7 ppm signal in CFH. c) Irradiation at δ = 2.7 ppm and δ = 3.3 ppm signals in CGH.

this parameter in sensibility of NOE phenomenon. In theory, according to the viscosity of these mixtures, NADES constituents in water are close to the second system described above, although when this parameter was optimized, the best NOEs were observed with the intermediate value of 0.7 s mixing time. Consequently, this mixing time value was set for the rest of the NOE experiments in the present work.

3.1.2. Dilution effects

Once we confirmed the spatial proximities between the NADES components, different dilutions of LGH, CFH and CGH in water were analyzed using the NOEs of ^{1}H NMR, in order to study the dilution effect in their intermolecular interactions.

Fig. 3 shows the ^{1}H NMR spectra recorded for dilutions of LGH. When H-3 signal from lactic acid was irradiated (Fig. 3a), 10% LGH was the only dilution which did not present NOE, indicating the existence of a limit value between 10% LGH and 20% LGH in which intermolecular interactions between glucose and lactic acid are lost. Furthermore, a reciprocal behavior was observed when the central region of glucose

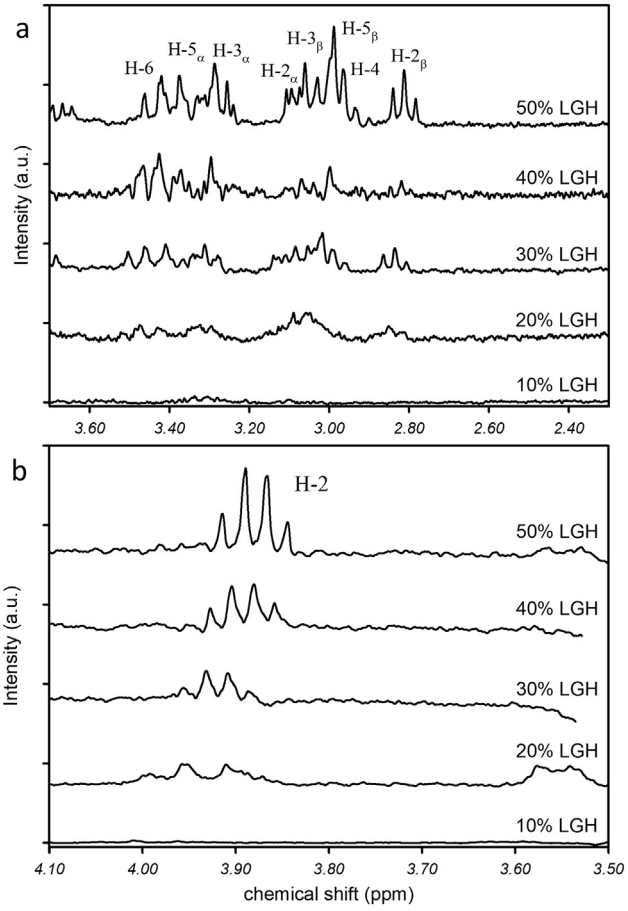

Fig. 3. Dilution effects registered for LGH in the NOE difference spectra. a) Irradiation at δ = 1.2 ppm proton signal. b) Irradiation at δ = 3.6 ppm signal.

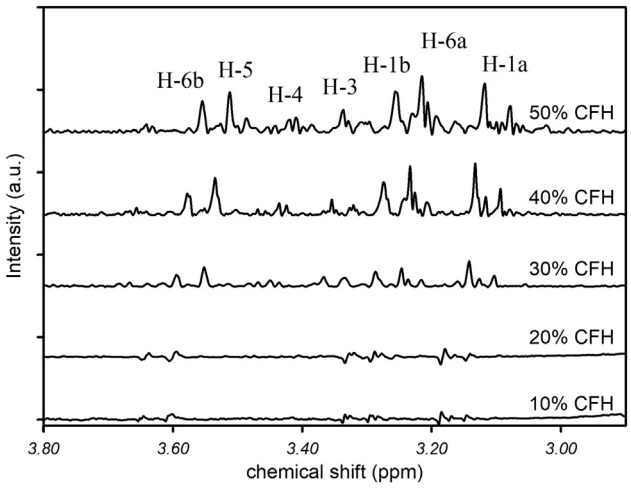

Fig. 4. Dilution effects registered for CFH in the NOE difference spectrum when proton signal at δ = 2.7 ppm was irradiated.

was irradiated (δ = 3.30 ppm, Fig. 3b); i.e., NOEs effects were observed from 20% LGH.

The NOEs registered for the dilutions of CFH are shown in the ^{1}H NMR spectra of Fig. 4. In this case, when the proton signals from citric acid were irradiated, 30%, 40% and 50% CFH presented the NOE effect. Accordingly, it seems that the frontier value in which intermolecular interactions decrease lies within 20% and 30% CFH. Specific care is needed regarding the presence of fructose signals in ^{1}H NMR spectra analyzed for 10% CFH and 20% CFH. These signals are clearly artifacts

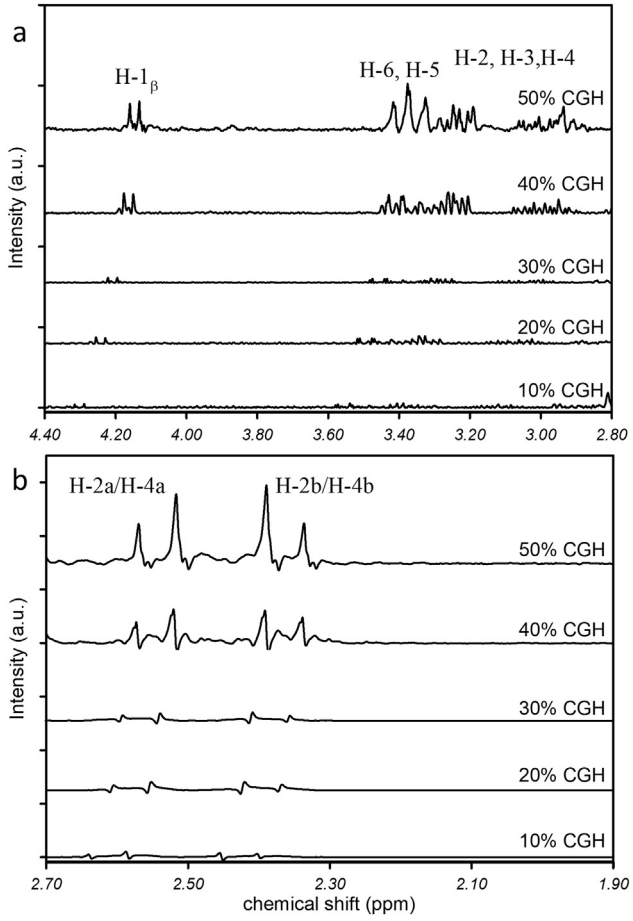

Fig. 5. Dilution effects registered for CGH in the NOE difference spectra. a) Irradiation at δ = 2.7 ppm proton signal. b) Irradiation at δ = 3.3 ppm signal.

from the technique instead of a real NOE effect. The two kinds of artifacts most commonly seen in the NOE spectra are subtraction artifacts (instability in the deuterium lock) and *J* coupling artifacts (*J* coupling between the irradiated peak and the observed peak). Since the hydrogen atoms analyzed correspond to different molecules, there can be no *J* coupling artifacts. The instability in the deuterium lock cause the peak subtracted out to be unaligned with the positive peak; according to this, all the signals seem to be repeated upside-down and slightly offset from the positive peak, resulting in an antiphase pattern (Fig. 4, 10% and 20% CFH). Unlike the case of LGH, when the sugar moiety was irradiated in CFH (δ = 3.60 ppm, fructose), no NOE effects were observed in the ^{1}H NMR spectra.

Finally, the ^{1}H NMR spectra recorded for dilutions of CGH are shown in Fig. 5. Through the irradiation of the signal at δ = 2.7 ppm from citric acid (Fig. 5a), dilutions beginning with 40% CGH presented NOE effects by the appearance of most signals from the glucose carbinolic hydrogens (H-1$_\beta$, H-2, H-3, H-4 and H-5). Moreover, when the central region of glucose protons was irradiated at δ = 3.3 ppm (Fig. 5b), NOE effects were observed for 40% and 50% CGH by the occurrence of the citric acid double-doublet signal. As can be expected in ^{1}H NMR when varying concentrations, the dilution effects also produce chemical shifts with higher δ values. Therefore, in Figs. 3 to 5, a slightly different position from the same signal between the ^{1}H NMR spectra was observed.

In summary, the dilutions of LGH, CFH and CGH analyzed by ^{1}H NMR confirmed the spatial proximity between the hydrogen atoms of the different NADES constituents. NOE effects were observed in several of these dilutions, being LGH the solvent with the best outcome among the higher dilutions. According to these dilution effects, thresholds

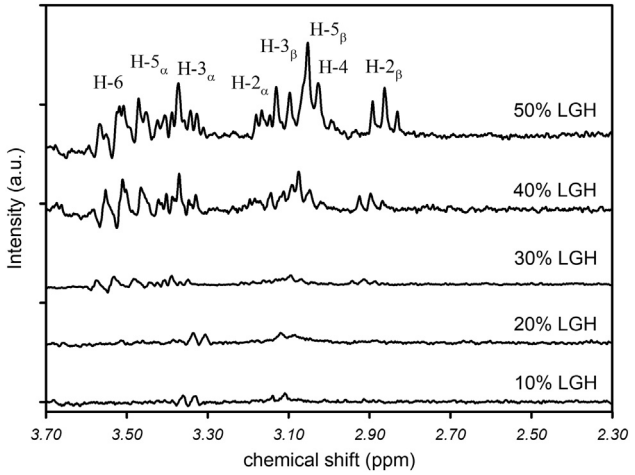

Fig. 6. NOE difference registered from the ^{1}H NMR spectra of the 10 mg L^{-1} quercetin solutions in LGH when lactic acid (δ = 1.20 ppm) signal were irradiated.

could be established for each NADES in which the supramolecular structure is lost. These thresholds would be between 10 and 20% for LGH, 20–30% for CFH, and 30–40% for CGH.

3.1.3. NADES solvation effect

In order to study whether the NADES supramolecular structure are affected when the solvents are in contact with certain analytes, QR was added to the LGH dilutions (50–90%) to reach a 10 mg L^{-1} QR solution in the corresponding dilutions. LGH was selected because it showed the largest NOE effects through the dilutions. The analyte evaluated was QR, considering that it is the most common flavonoid widespread in plants and a major bioflavonoid in the human diet. In addition, interactions between QR and glucose-choline chloride based NADES has been previously confirmed, showing that QR has strong interaction with the structure of the natural solvent [4]. Fig. 6 shows the ^{1}H NMR spectra obtained when these dilutions were irradiated at the same previously studied proton signals (i.e., lactic acid signal at δ = 1.20 ppm).

As mentioned in Section 3.1.2, when the ^{1}H NMR spectra were recorded for LGH dilutions, multiple NOEs were observed, and only 10% LGH showed no NOE effect by irradiation of lactic acid and glucose signals. However, when quercetin was added, NOEs were registered only for 40% and 50% LGH. These observations indicate that the interaction between QR and LGH is strong enough to perturb the intermolecular interactions present in diluted solutions of LGH (20% and 30% LGH).

3.2. Theoretical study

Simultaneously with the experimental study of NADES by ^{1}H NMR, a molecular modelling in solution of the systems LGH, CFH and CGH was performed. This theoretical study was carried out in order to rationalize the presence of intermolecular interactions found between NADES components. Fig. 7 shows the geometries of the three systems optimized in water at the M06-2X/6-31 + G(d,p) level of theory. The optimized geometries were ca. 2 Kcal/mol more stable than the rest of conformations found for each system (1.86, 2.04 and 2.31 Kcal/mol for LGH, CFH and CGH respectively).

In the case of LGH, the conformation obtained after geometry optimization presents two interactions of the hydrogen bond type (Fig. 7a), namely one interaction between the oxygen bonded to C-6 from glucose and the hydrogen of the hydroxyl group from lactic acid (1.83 Å, Fig. 7a-1), and another interaction between the hydrogen of the hydroxyl group of C-4 from glucose and the oxygen atom of the

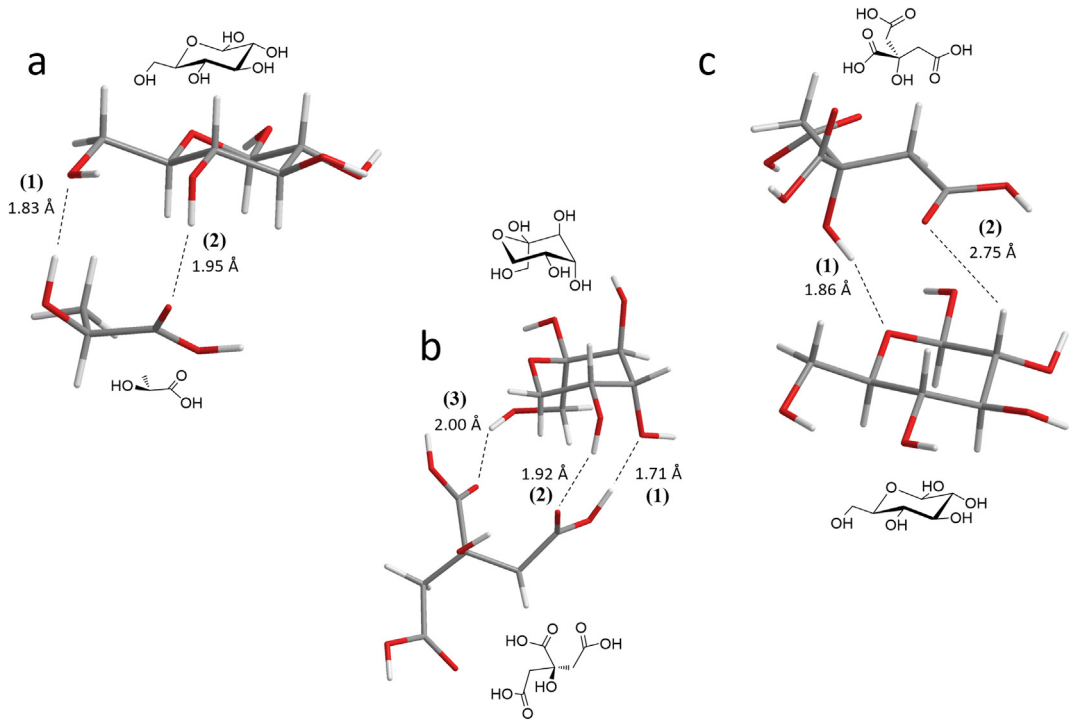

Fig. 7. Optimized geometries of NADES in water at M06-2X/6-31G + (d,p) level of theory. a) LGH. b) CFH. c) CGH.

carbonyl group from lactic acid (1.95 Å, Fig. 7a-2).

On the other hand, the optimized geometry for the CFH system yielded three hydrogen bond interactions (Fig. 7b). The minimum distance between a hydrogen atom and the acceptor was between the hydrogen of the hydroxyl from the carboxylic group of citric acid and the oxygen bonded to C-4 from fructose (1.71 Å, Fig. 7b-1). A second interplay was between the hydrogen of the hydroxyl group of C-5 from fructose and the oxygen atom of carbonyl group from citric acid (1.92 Å, Fig. 7b-2). The third interaction in CFH was observed between the hydrogen of the hydroxyl group of C-1 from fructose and the oxygen atom from another carbonyl group in citric acid (2.00 Å, Fig. 7b-3).

Finally, the conformation obtained for CGH after geometry optimization is shown in Fig. 7c. In this case, two interactions of hydrogen bond type emerged: one interplay between the hydrogen of the hydroxyl group from citric acid and the oxygen from the glucopyranosyl ring from glucose (1.86 Å, Fig. 7c-1), and a second unconventional hydrogen bond between H-2 from glucose and the oxygen atom from carbonyl group in citric acid (2.75 Å, Fig. 7c-2).

Additional information obtained during the theoretical study of the NADES is summarized in Table 1. Although the Wiberg index is not directly applicable to ab-initio wavefunctions, its values are usually very close to the formal bond order. Using the Wiberg index together with second order perturbation theory, it is possible to estimate the strength in a non-covalent interaction. Only the main interactions are detailed. Furthermore, Table 1 collects the energies of stabilization through hydrogen bond formation (absolute energies including zero-point energy correction in Kcal/mol), which are related to the stability of NADES according to their intermolecular interactions. In addition, Table 1 also shows specific bonding energies E(2) associated with delocalization of electrons according to second order perturbation theory analysis of Fock matrix in the NBO basis [30].

As can be seen in Table 1, most of the hydrogen bonds emerged from the interaction between lone pairs of electrons (LP) from oxygen atoms and antibonding orbitals (BD*) of the H—O bond from hydroxyl groups. Three hydrogen bonds were observed for CFH, while LGH and CGH presented only two interactions. In the three studied systems, strong intermolecular interactions of the hydrogen bonding type with

Table 1
Wiberg bond indexes and second order perturbation theory analysis of Fock matrix in Natural Bond Orbital (NBO) basis. a: Absolute energies including zero-point energy correction ($\Delta E = E_{dimer} - E_{isolated\ monomers}$). b: Specific bonding energies E(2) associated with delocalization of electrons according donor-acceptor NBO orbital interactions. LP: lone pair electrons; BD: bonding orbital; BD*: antibonding orbital. glu: glucose; fru: fructose; lac: lactic acid; cit: citric acid.

	ΔE[a] (Kcal/mol)	Distance (Å)	Wiberg index	Donor NBO	Acceptor NBO	E(2)[b] (Kcal/mol)
LGH	−8.57	1.83	0.0540	O (LP)^{glu}	H–O (BD*)^{lac}	17.48
		1.95	0.0243	O (LP)^{lac}	H–O (BD*)^{glu}	6.81
CFH	−10.51	1.71	0.0677	O (LP)^{fru}	H–O (BD*)^{cit}	25.53
		1.92	0.0351	O (LP)^{cit}	H–O (BD*)^{fru}	6.63
		2.00	0.0218	O (LP)^{cit}	H–O (BD*)^{fru}	5.42
CGH	−7.74	1.86	0.0424	O (LP)^{glu}	H–O (BD*)^{cit}	14.11
		2.75	0.0024	H–O (BD)^{cit}	H–O (BD*)^{glu}	1.04

distances between 1.71 and 2.75 Å were recorded. Furthermore, these interactions present complementary bonds, i.e., each constituent of the NADES has a hydrogen bond donor and a hydrogen bond acceptor. The negative energy values obtained by the dimeric modelled systems confirm the stabilization achieve by the intermolecular interactions. In concordance with the number of hydrogen bonds find for each system, the highest stabilization (highest ΔE in absolute value) was achieved for CFH system, while CGH system yield the lowest stabilization by hydrogen bond formation (one of the interaction was an unconventional hydrogen bond).

In summary, all the modelled structures of the NADES confirmed the spatial proximities that allow through-space interactions between the components, as registered in the NOEs observed in ^{1}H NMR spectra. In agreement with the experimental study, the molecular modelling confirmed the existence of hydrogen bonding interactions for the LGH, CGH and CFH systems. According to the number of interactions and the stabilization energies predicted for each NADES, CFH should in principle be the strongest NADES in holding the supramolecular structure

across the dilutions. Nevertheless, the experimental evidence found in the ^{1}H NMR spectra showed otherwise, i.e., LGH is apparently the NADES that best holds its supramolecular structure throughout the dilutions. Although the proposed model was able to find intermolecular interactions among the NADES, it partially failed to predict which of the three systems under study should have a stronger supramolecular structure. This is probably due to the fact that the real system could contain a network of organic acids and monosaccharides interacting with each other simultaneously, which would be impossible to model due to the computational times associated with the level of theory employed in this study.

4. Conclusions

A theoretical and experimental study was performed on three NADES, namely, LGH, CFH and CGH. Intermolecular interactions between NADES components were experimentally confirmed by the presence of multiple NOE effects in the analysis of ^{1}H NMR spectra. In addition, the dilutions of LGH, CFH and CGH also confirmed the spatial proximity between several hydrogen atoms of the different NADES constituents. NOE effects were observed in many of these dilutions, LGH being the solvent with the best outcome throughout the dilutions. In solutions containing quercetin and LGH, an attenuation in the NOE effect was observed, indicating that the interaction between LGH and the analyte was strong enough to modify the LGH structure for the highest dilutions. In agreement with the experimental evidence, a simplified dimeric model of the NADES in the theoretical study reproduced the spatial proximity between their components. Furthermore, the calculations allowed rationalizing the intermolecular interactions by finding at least two complementary hydrogen bonds between the components of every NADES.

Acknowledgements

We gratefully acknowledge the financial support from Universidad Nacional de Rosario, Universidad Nacional de Cuyo, CONICET (Consejo Nacional de Investigaciones Científicas y Técnicas) and ANPCyT (Agencia Nacional de Promoción Científica y Tecnológica, Project PICT-2015-1471). We would like to thank the staff from the English Department (Facultad de Ciencias Bioquímicas y Farmacéuticas, UNR) for the language correction of the manuscript.

References

[1] M. Espino, M. de los Ángeles Fernández, F.J.V. Gomez, M.F. Silva, Natural designer solvents for greening analytical chemistry, Trends Anal. Chem. 76 (2016) 126–136.
[2] D. Rengstl, V. Fischer, W. Kunz, Low-melting mixtures based on choline ionic liquids, Phys. Chem. Chem. Phys. 16 (2014) 22815–22822.
[3] M. Cvjetko Bubalo, S. Vidović, I. Radojčić Redovniković, S. Jokić, New perspective in extraction of plant biologically active compounds by green solvents, Food Bioprod. Process. 109 (2018) 52–73.
[4] Y. Dai, J. van Spronsen, G.-J. Witkamp, R. Verpoorte, Y.H. Choi, Natural deep eutectic solvents as new potential media for green technology, Anal. Chim. Acta 766 (2013) 61–68.
[5] M.C. Gutiérrez, M.L. Ferrer, C.R. Mateo, F. del Monte, Freeze-drying of aqueous solutions of deep eutectic solvents: a suitable approach to deep eutectic suspensions of self-assembled structures, Langmuir 25 (2009) 5509–5515.
[6] F.J.V. G., E. Magdalena, F.M. A., M.F. S., A greener approach to prepare natural deep eutectic solvents, ChemistrySelect 3 (2018) 6122–6125.
[7] Y. Liu, J.B. Friesen, J.B. McAlpine, D.C. Lankin, S.-N. Chen, G.F. Pauli, Natural deep eutectic solvents: properties, applications, and perspectives, J. Nat. Prod. 81 (2018) 679–690.
[8] A. Shishov, A. Bulatov, M. Locatelli, S. Carradori, V. Andruch, Application of deep eutectic solvents in analytical chemistry. A review, Microchem. J. 135 (2017) 33–38.
[9] F. Aydin, E. Yilmaz, M. Soylak, A simple and novel deep eutectic solvent based ultrasound-assisted emulsification liquid phase microextraction method for malachite green in farmed and ornamental aquarium fish water samples, Microchem. J. 132 (2017) 280–285.
[10] P. Li, P. Zhao, W. Liu, Y. Jiang, W. Wang, L. Bao, Y. Jin, X. Li, Determination of common ginsenosides in Kang'ai injection by aqueous two-phase extraction with deep eutectic solvents and HPLC-UV/DAD, Microchem. J. 137 (2018) 302–308.
[11] Y. Dai, G.-J. Witkamp, R. Verpoorte, Y.H. Choi, Tailoring properties of natural deep eutectic solvents with water to facilitate their applications, Food Chem. 187 (2015) 14–19.
[12] A. Paiva, R. Craveiro, I. Aroso, M. Martins, R.L. Reis, A.R.C. Duarte, Natural deep eutectic solvents – solvents for the 21st century, ACS Sustain. Chem. Eng. 2 (2014) 1063–1071.
[13] R. Xin, S. Qi, C. Zeng, F.I. Khan, B. Yang, Y. Wang, A functional natural deep eutectic solvent based on trehalose: structural and physicochemical properties, Food Chem. 217 (2017) 560–567.
[14] M.d.l.Á. Fernández, M. Espino, F.J.V. Gomez, M.F. Silva, Novel approaches mediated by tailor-made green solvents for the extraction of phenolic compounds from agro-food industrial by-products, Food Chem. 239 (2018) 671–678.
[15] F.J.V. Gomez, M. Espino, M. de los Angeles Fernandez, J. Raba, M.F. Silva, Enhanced electrochemical detection of quercetin by Natural Deep Eutectic Solvents, Anal. Chim. Acta 936 (2016) 91–96.
[16] F.J.V. Gomez, A. Spisso, M. Fernanda Silva, Pencil graphite electrodes for improved electrochemical detection of oleuropein by the combination of Natural Deep Eutectic Solvents and graphene oxide, Electrophoresis 38 (2017) 2704–2711.
[17] N.E. Jacobsen, NMR Data Interpretation Explained: Understanding 1D and 2D NMR Spectra of Organic Compounds and Natural Products, Wiley, Hoboken, New Jersey, 2016.
[18] W.L.F. Armarego, Purification of Laboratory Chemicals, Eighth ed., Elsevier Inc., Amsterdam, Netherlands, 2017.
[19] https://www.bruker.com/fileadmin/user_upload/8-PDF-Docs/MagneticResonance/NMR/brochures/AViiihd_nano_200-400_specs.pdf.
[20] Hyperchem Professional Release 7.52, (2005).
[21] Y. Zhao, D. Truhlar, The M06 suite of density functionals for main group thermochemistry, thermochemical kinetics, noncovalent interactions, excited states, and transition elements: two new functionals and systematic testing of four M06-class functionals and 12 other functionals, Theor. Chem. Accounts 120 (2008) 215–241.
[22] M.J. Frisch, G.W. Trucks, H.B. Schlegel, G.E. Scuseria, M.A. Robb, J.R. Cheeseman, G. Scalmani, V. Barone, B. Mennucci, G.A. Petersson, H. Nakatsuji, M. Caricato, X. Li, H.P. Hratchian, A.F. Izmaylov, J. Bloino, G. Zheng, J.L. Sonnenberg, M. Hada, M. Ehara, K. Toyota, R. Fukuda, J. Hasegawa, M. Ishida, T. Nakajima, Y. Honda, O. Kitao, H. Nakai, T. Vreven, J.A. Montgomery Jr., J.E. Peralta, F. Ogliaro, M.J. Bearpark, J. Heyd, E.N. Brothers, K.N. Kudin, V.N. Staroverov, R. Kobayashi, J. Normand, K. Raghavachari, A.P. Rendell, J.C. Burant, S.S. Iyengar, J. Tomasi, M. Cossi, N. Rega, N.J. Millam, M. Klene, J.E. Knox, J.B. Cross, V. Bakken, C. Adamo, J. Jaramillo, R. Gomperts, R.E. Stratmann, O. Yazyev, A.J. Austin, R. Cammi, C. Pomelli, J.W. Ochterski, R.L. Martin, K. Morokuma, V.G. Zakrzewski, G.A. Voth, P. Salvador, J.J. Dannenberg, S. Dapprich, A.D. Daniels, Ö. Farkas, J.B. Foresman, J.V. Ortiz, J. Cioslowski, D.J. Fox, Gaussian 09W, Gaussian, Inc., Wallingford, CT, USA, 2009.
[23] Y. Zhao, D.G. Truhlar, Density functionals with broad applicability in chemistry, Acc. Chem. Res. 41 (2008) 157–167.
[24] A.V. Marenich, C.J. Cramer, D.G. Truhlar, Universal solvation model based on solute electron density and on a continuum model of the solvent defined by the bulk dielectric constant and atomic surface tensions, J. Phys. Chem. B 113 (2009) 6378–6396.
[25] J. Tomasi, B. Mennucci, R. Cammi, Quantum mechanical continuum solvation models, Chem. Rev. 105 (2005) 2999–3094.
[26] E.D. Glendening, C.R. Landis, F. Weinhold, Natural bond orbital methods, Wiley Interdiscip. Rev.: Comput. Mol. Sci. 2 (2012) 1–42.
[27] T.L. Mega, S. Cortes, R.L. Van Etten, The oxygen-18 isotope shift in carbon-13 nuclear magnetic resonance spectroscopy. 13. Oxygen exchange at the anomeric carbon of D-glucose, D-mannose, and D-fructose, J. Org. Chem. 55 (1990) 522–528.
[28] A. De Bruyn, M. Anteunis, G. Verhegge, A 1H-n.m.r. study of D-fructose in D2O, Carbohydr. Res. 41 (1975) 295–297.
[29] S.J. Angyal, The composition of reducing sugars in solution: current aspects, in: D. Horton (Ed.), Advances in Carbohydrate Chemistry and Biochemistry, Academic Press, 1991, pp. 19–35.
[30] E.D. Glendening, A.E. Reed, J.E. Carpenter, F. Weinhold, NBO Version 3.1. Theoretical Chemistry Institute, University of Wisconsin, Madison, 1998.